Journal of Power Sources 256 (2014) 324–328

Contents lists available at ScienceDirect

Journal of Power Sources

journal homepage: www.elsevier.com/locate/jpowsour

Short communication

In situ surface enhanced Raman spectroscopic studies of solid electrolyte interphase formation in lithium ion battery electrodes

Sunny Hy [a,1], Felix [a,1], Yi-Hsiu Chen [a], Jyong-yue Liu [a], John Rick [a], Bing-Joe Hwang [a,b,*]

[a] Nanoelectrochemistry Laboratory, Department of Chemical Engineering, National Taiwan University of Science and Technology, Taipei, Taiwan
[b] National Synchrotron Radiation Research Center, Hsin-Chu, Taiwan

HIGHLIGHTS

- In situ surfaced-enhanced Raman spectroscopy study on a Si electrode for lithium ion battery.
- Observation of solid electrolyte interphase growth during discharge.
- Comparison of normal Raman and SERS shows varying degrees of lithiation for the bulk and surface.

GRAPHICAL ABSTRACT

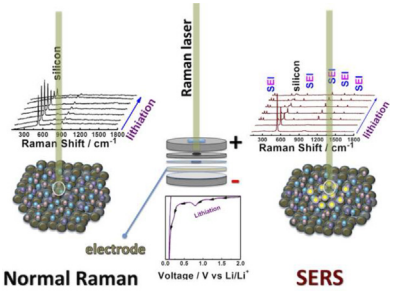

ARTICLE INFO

Article history:
Received 9 November 2013
Received in revised form
10 January 2014
Accepted 20 January 2014
Available online 28 January 2014

Keywords:
Lithium battery
Raman
Surfaced-enhanced Raman spectroscopy
Solid electrolyte interphase
In situ

ABSTRACT

The use of surfaced-enhanced Raman spectroscopy (SERS) in lithium-ion battery (LIB) and Li–O_2 battery studies has proven to be a powerful tool for observing solid electrolyte interphase (SEI) growth, on the electrode's surface, that is crucial in determining the battery's electrochemical performance. Here, we report the use of SiO_2-coated Au nanoparticles for *in situ* SERS studies during electrochemical cycling to directly observe SEI formation on the electrode. The comparison of silicon electrodes with and without the electrolyte additive vinylene carbonate (VC) shows the formation of VC-related reduction products on the electrode's surface before the reduction of ethylene carbonate. Further observation, using normal Raman and SERS, of the silicon band intensity shows different amorphization rates between bulk and surface. These successful proof-of-concept experiments should allow this technique to be extended to other electrode material studies in conjunction with other surface sensitive techniques to further our understanding of surface reactions that heavily influence overall battery performance.

1. Introduction

Under normal battery operating conditions, the solid electrolyte interphase (SEI) is formed on the electrode, during the initial cycle, due to the reduction of non-aqueous electrolyte. Considered highly complex and varying with both electrolytes and electrodes used, SEI characterization is often difficult because such interfaces are intrinsically thin and non-uniform. Raman and Surface-enhanced Raman spectroscopy (SERS) with Ag or Au electrodes has been successfully employed to probe the structural transformation, or state changes, of these thin film electrodes [1–3] and also to observe SEI components in different electrolyte systems [4–8]. Although these experiments have given insights into the role of stable components in varying electrolyte systems, they do not take into account the contribution from the electrode material (i.e. carbon, Si, Sn, etc.). For example, carbon and silicon-based anodes have differing intercalation/deintercalation mechanisms, varying

* Corresponding author. Tel.: +886 2 2737 6624; fax: +886 2 27376644.
E-mail address: bjh@mail.ntust.edu.tw (B.-J. Hwang).
[1] These two authors contributed equally.

0378-7753/$ – see front matter © 2014 Elsevier B.V. All rights reserved.
http://dx.doi.org/10.1016/j.jpowsour.2014.01.092

anode reactions, and material-dependent volume expansions that govern their respective SEIs [9,10]. Therefore, to imply that the stated use of Ag or Au electrodes conveys useful information about the nature of the resulting SEI may be an oversimplification. Shell-isolated nanoparticle (NP)-enhanced Raman spectroscopy (SHINERS) utilizes the ultra-sensitive properties of SERS by employing NP probes with ultrathin coatings in a passive non-destructive technique that does not lead to agglomeration [11,12]. The NPs can be directly applied to the surface of the electrode to allow the study of SEIs with different electrode materials. In this study we report the first *in situ* SERS study of a nano-Si anode (~100 nm), during the first discharge cycle, giving us an insight into SEI formation and the accompanying silicon morphological changes.

2. Experimental

2.1. Au@SiO_2 nanoparticle preparation

Au NPs (diameter ~35–40 nm) were synthesized by a standard sodium citrate reduction method [12]. Briefly, (3-Aminopropyl) trimethoxysilane (1 mM) was added to the sol under vigorous magnetic stirring followed by the addition of 0.54 wt% sodium silicate solution. The washed and dried Au@SiO_2 NPs were transferred to an Ar-filled glove box and re-dispersed in diethyl carbonate (DEC). Silicon electrodes were fabricated with a ~100 nm Si:Super P carbon:Polyvinylidene fluoride binder (weight ratio 80:10:10) composition made into a slurry using *N*-methyl-2-pyrrolidone and then cast over a Cu foil which was then dried in a vacuum oven at 80 °C overnight.

2.2. Electrochemical and in situ SERS measurements

A commercial electrolyte comprising of ethylene carbonate/diethyl carbonate (EC/DEC) 1:1 with added $LiPF_6$ (1 M) and a separate commercial electrolyte comprising of an addition 2 wt% VC was used in a half-cell 2032 coin cell-type battery with a Li foil counter electrode and Si or Cu anode. The Si electrodes were cycled at 0.1 C from 1 to 0.05 V while the Cu foil was discharged to 0 V and held for 5 h. For *in situ* measurements, the Au@SiO_2 NPs were dripped onto the electrode, dried and the coin cell assembled. A quartz window (0.17 mm thick) was applied to the coin cell and a small hole made through the top cap, lithium foil and separator. *In situ* cyclic voltammetry (CV) measurements were made using an Autolab Potentiostat running at 0.5 mV s^{-1} from the open circuit potential (OCV) to 0.0 V where the potential was held to allow the current to drop before each measurement. *Ex situ* measurements of the Cu foil was done after extracting, cleaning, and drying the electrode with DEC then placing in a sealed holder with a thin quartz window.

Raman micro-spectroscopy measurements were performed on the ProMaker system mounted with one TE cooled CCD of 1024 × 256 pixels as integrated by Protrustech Corporation Limited. The system with a 50× long working distance lens (Olympus America inc.) was operated at an excitation wavelength of 532 nm, with ~1 mW power, in order to avoid any electrode surface degradation. The exposure time was 5 s with 10 accumulations.

3. Results and discussion

3.1. Au@SiO_2 characterization

The Au NPs in this study are between 30 and 40 nm in diameter, while the thickness of the SiO_2 coating is ~ 3–5 nm as shown in the TEM images in Fig. 1. The SiO_2 coating serves two main purposes: to avoid agglomeration, and to isolate the Au nanoparticles from the

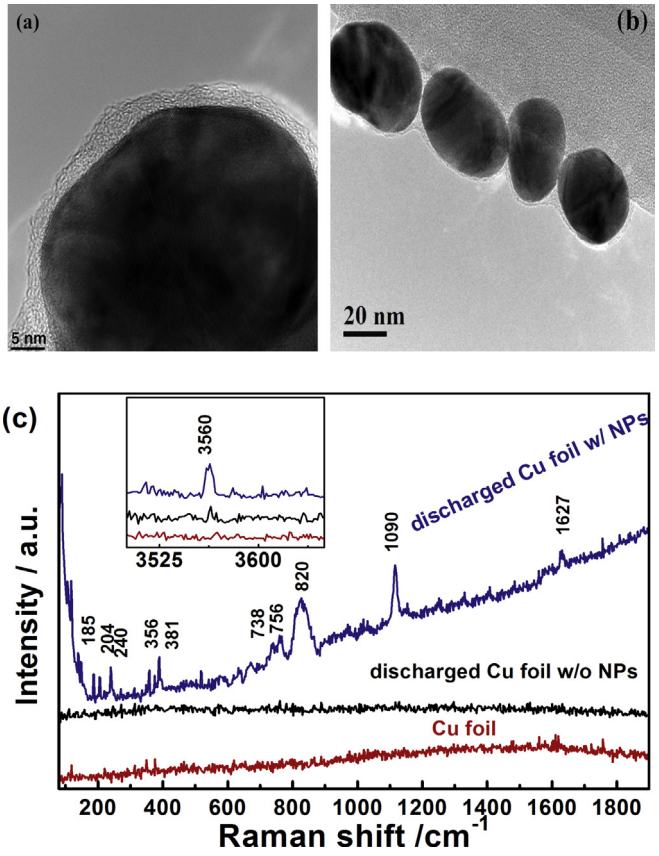

Fig. 1. (a) and (b) showing the TEM images of the SiO_2-coated Au nanoparticle. (c) is the Raman spectra foil Cu foil, electrochemically discharged Cu foil with and without nanoparticles. Inset shows the higher range for the Raman shift.

substrate, which in this case is a Li-ion battery electrode. The surface enhancement of SEI from the Au@SiO_2 NPs was evaluated by applying the NPs to a Cu foil anode that was short-circuited, or lithium-plated (electrochemically discharged to 0 V) for several hours, in a battery to form an SEI layer from the reduction of the electrolyte. Fig. 1(c) shows the Raman spectra from the Cu foil and the Cu foil after being short-circuited with and without NPs. The Cu foil and discharged Cu foil without NPs shows similar spectra with no bands being observed.

In contrast, several bands are present on the discharged Cu foil with NPs. These bands can be assigned to the reduction products of the electrolyte that agree well with an *ex situ* SERS study performed on a similar non-aqueous electrolyte on a roughened Ag electrode [4]. In particular, the bands at 356, 381, 820 and 3650 (inset) cm^{-1} correspond to $LiOH{\cdot}H_2O$ and the bands at 204, 738, 756, and 1090 cm^{-1} correspond to Li_2CO_3. For further comparison, Schmitz et al., [7] have performed a SEI investigation on lithium-plated Cu electrodes using normal Raman spectroscopy noting broad bands at 470 and 920 cm^{-1} and also bands corresponding to Li_2CO_3 (one band at 1080 cm^{-1}) and Li_2C_2 (1856 cm^{-1}) that was suggested to be observable due to possible surface enhancement. However, unlike this present work and the work done by Li et al. [4,5], $LiOH{\cdot}H_2O$ and multiple Li_2CO_3, bands were not observed. This may be due to the weaker surface enhancement, which may have a dependence on the size of the Li plated. This is analogous to the dependence of nanoscale Li–Ag alloys for the Ag electrode. Li_2C_2 was not observed in this present study even after probing different points on the electrode. Further investigation is needed to understand the difference. It is believed the two lower bands within the Schmitz's work most likely belong to residual electrolyte solvent. The

enhancement of surface species bands suggests that the Au@SiO_2 NPs are suitable for observing SEI layers and may be used to study other electrode materials' surfaces.

3.2. Electrochemical evaluation

Silicon shows great promise as an anode material for LIB due to its large theoretical capacity (4200 mAh g^{-1}) [13]. However, silicon undergoes a large first irreversible capacity change and a large volume expansion that serves to pulverize and electronically isolate silicon particles upon lithiation. Different strategies have been developed to overcome these issues. One includes modification of the electrolyte by the addition of small concentrations of additives that serve to restructure the SEI layer composition. Vinylene carbonate (VC) has been found to substantially increase stability within silicon film anodes due to the formation of a smooth, more elastic and LiF-deficient SEI that shows less resistance towards Li^+ [14]. The formation of this better SEI owes to the initial reduction of VC through a radical polymerization reaction to form poly (VC) before the reduction of the less stable SEI from EC reduction. In order to eliminate complexities of composite materials with variable intercalation, we used silicon anodes that consist mostly of silicon (80 wt%) and only small amounts of conductive carbon (10wt%) to observe changes during lithiation. Fig. 2 shows the electrochemical performance of the silicon anode during galvanostatic charging and discharging. While the performance of both batteries is not comparable to that of other silicon-based batteries [13,15], the addition of 2 wt% VC shows an improvement in the first cycle irreversible capacity and cycle stability as shown in Fig. 2(a) and (b), respectively. Fig. 2(c) shows cyclic voltammograms (CV) where a reduction peak at ~1.5–1.1 V for the VC-containing battery corresponds to the reduction of VC. A peak at ~0.8 V for both batteries is observed corresponding to the reduction of ethylene carbonate (EC). This corresponds well with the onset of VC reduction occurring before EC within a graphite anode system [16]. However, unlike with a graphite anode, the reduction of EC was still prevalent with or without the addition of VC for the silicon anode.

3.3. In situ Raman and SERS measurements

To observe the formation of SEI layers for normal and VC-containing electrolytes and the evolution of the silicon anode, *in situ* normal Raman (NR) and SERS were performed during electrochemical CV. Fig. 3 shows the *in situ* NR spectra and *in situ* SERS for normal (a) and (c) and VC-containing electrolytes (b) and (d), respectively. For NR, the evolution of the silicon band at ~530 cm^{-1} shows a drop in intensity with decreasing voltage. For both systems, a slight fluorescent effect can be observed upon lithiation due to the formation of SEI. Although this fluorescent effect is relatively different, the evolution of the silicon band intensity shows a similar trend. It should be noted that silicon under the current electrochemical conditions did not become fully amorphous as in other studies as indicated by the remaining band after discharge to 0 V [17,18]. Nevertheless, the evolution of the band indicates lithiation of silicon is occurring and is used to compare with the SERS spectra under the same electrochemical conditions. For SERS spectra, compared to NR spectra, extra bands can be seen to form with lithiation for both batteries.

For both SERS spectra, bands at 132,162, 199, 443, 698, 1094, 1315, and 1475 cm^{-1} are observed upon discharge to ~0.9 V where EC reduction generally takes place: most of these bands correspond with Li_2CO_3 [19,20]. For the VC-containing battery, an extra peak can be observed at ~1000 cm^{-1} is related to the R–O and C–C stretching modes of semicarbonates that may be related to the radical polymerization of VC [7,21–23]. This new band as well as most the bands observed in the commercial electrolyte, besides the bands at 132, 443, and 1315 cm^{-1}, appear at the onset of the VC reduction potential (~1.5 V). Similar to Li_2CO_3, the bands at 700,

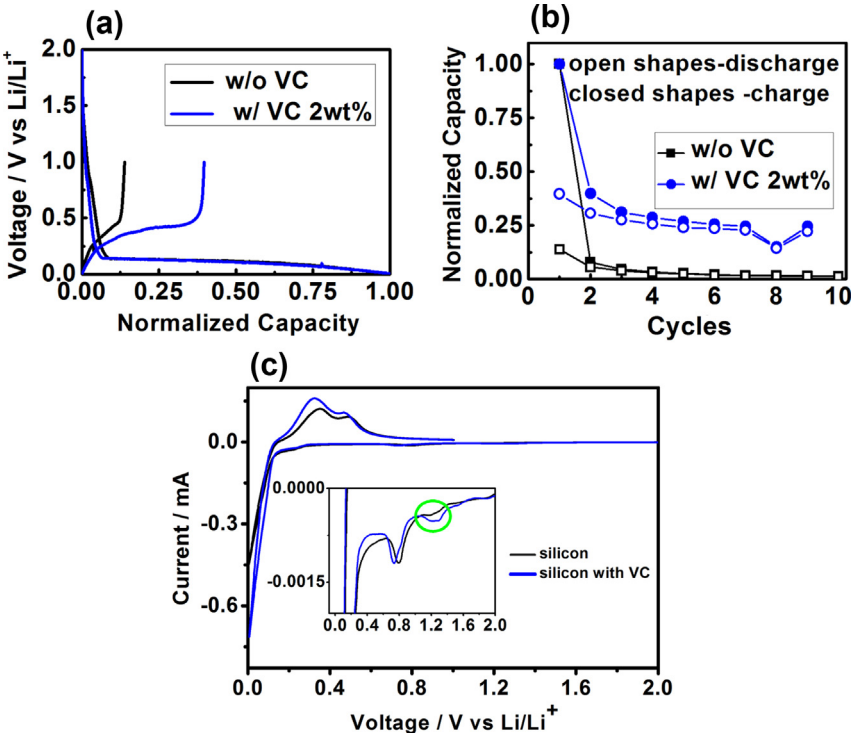

Fig. 2. (a) The first charging and discharging curve, (b) the normalized capacity versus cycles and (c) the CV curve with the inset that highlights the lithiation process. Green circle indicates VC reduction peak.

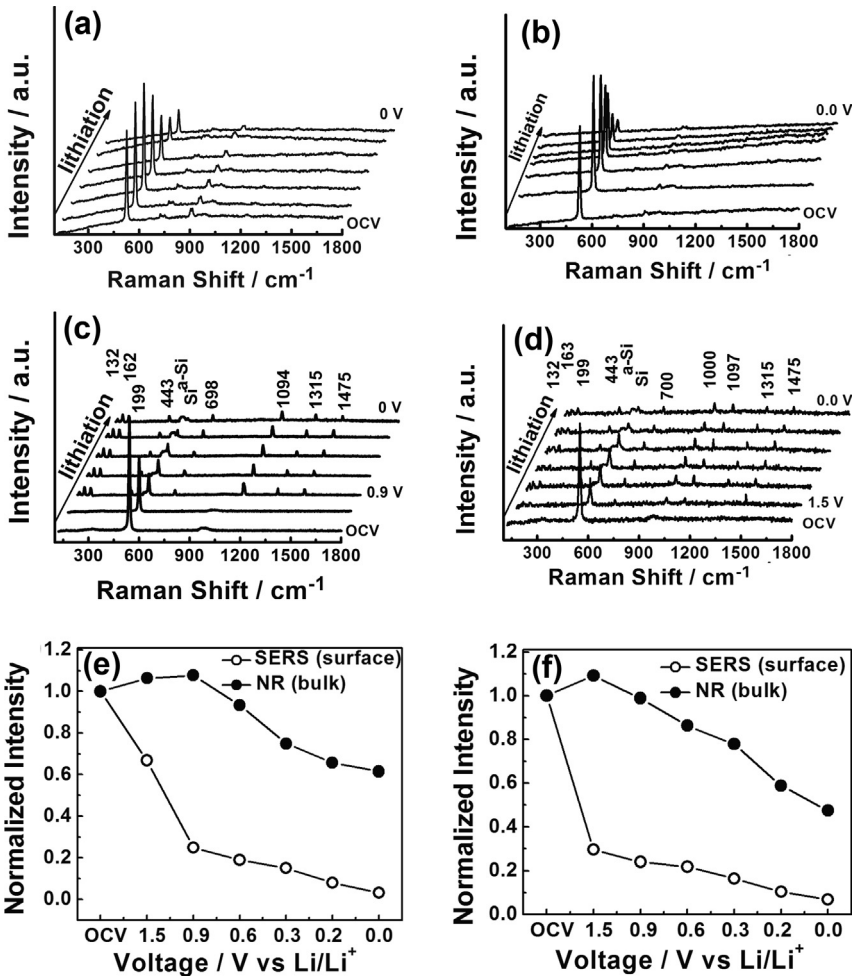

Fig. 3. *In situ* normal Raman spectroscopy without (a) and with (b) 2% vinylene carbonate and *in situ* surfaced-enhanced Raman spectroscopy without (c) and with (d) vinylene carbonate during lithiation/discharging. (e) and (f) is the normalized intensity of the silicon peak evolution with decreasing voltage for surface (SERS) and bulk (Raman).

1097, and 1475 cm^{-1} are assigned to the different vibration modes of CO_3^{2-} [19,20], which also may be related to the radical polymerization where a ring opening reaction would occur followed by the radical polymerization reaction [14,22,24,25]. However, by the *in situ* SERS technique alone, it is still not clear what specific species were formed due to the similarities of the functional groups in the VC reduction products that include lithium vinylene dicarbonate $(CHOCO_2Li)_2$, lithium divinylene dicarbonate $(CH{=}CHOCO_2Li)_2$, lithium divinylene dialkoxide $(CH{=}CHOLi)_2$, and lithium carboxylate (RCOOLi) [16,19,26]. Previously, Ota et al. [16] had employed a combination of FTIR, NMR, TOF-SIMS, XPS, and SEM in order to discern between the different species. In any case, it is clear that the addition of VC causes the formation of an additional band as well as the onset of several reductions products to occur (~1.5 V) before the reduction of EC (~0.9 V) leading to the superior cycle retention.

Amorphous silicon can also be observed (~480 cm^{-1}) starting at ~1 V for both SERS spectra and broadening with lithiation while, in contrast, the amorphous silicon band was not apparent within either of the NR spectra. Moreover, the silicon band showed a differing intensity of evolution during lithiation from that of the NR silicon band. The evolution of the normalized band intensity (normalized to the OCV silicon band intensity) was plotted versus the voltage and can be seen in Fig. 3(e) and (f) for normal and VC-containing batteries, respectively. The NR spectra, representing what is mostly the bulk material, shows similar evolution but the highest intensity is shown to occur at 0.9 V and 1.5 V for normal and VC-containing batteries, respectively. The SERS spectra show a relatively higher decrease in the intensity at 0.9 V for the normal battery and 1.5 V for the VC-containing battery this corresponds well with the CV and observation of the reduction product bands within the spectra. The amorphization of the surface (lithiation) also is seen to occur at a faster rate compared to the bulk evidenced by the rate of the intensity drop and amorphous silicon band appearance. This may imply that although the silicon particles used in this report were nano-sized, the lithiation process from surface to bulk is non-uniform. Attempts at plotting the evolution of the SEI product band intensities showed little to no change. Work is being done to test this system under various electrochemical conditions and exploration of other nanoparticles coated with inert coatings is under way. In addition, we are now in the process of more detailed analysis of this system (half and full-cell configuration) as well as other systems using the described *in situ* SERS coupled with other spectroscopic techniques to describe more clearly the specific species forming and reacting during electrochemical cycling.

4. Conclusions

To summarize; the experiments described in this report demonstrate the feasibility of using thin SiO_2-coated Au nanoparticles to observe SEI species formation and evolution at the electrode's surface material during electrochemical discharge – thereby allowing direct comparison with the bulk when coupled

with NR measurements. The observation of Raman bands corresponding to reduction products during electrochemical discharging on nano-sized silicon agrees well with the reduction peaks within the CV curve where an additional band was also observed for the VC containing electrolyte. The silicon band intensity evolution shows the amorphization of surface silicon taking place at a faster rate compared to the bulk. Coupled with other spectroscopic techniques, this technique can be further extended to other anode and cathode systems to elucidate crucial surface reactions, which ultimately determine the overall battery performance.

Acknowledgment

The financial supports from the National Science Council (NSC) (101-3113-E-011-002, 101-2923-E-011-001-MY3), the Ministry of Economic Affairs (MOEA) (101-EC-17-A-08-S1-183), and the Top University Projects of Ministry of Education (MOE) (101H451401), as well as the facilities supports from the National Taiwan University of Science and Technology (NTUST) are acknowledged. Damien S. Clark and Hening Marlistya Citraningrum for their helpful discussion and support.

References

[1] M. Moskovits, J. Raman Spectrosc. 36 (2005) 485–496.
[2] Y.-C. Liu, B.-J. Hwang, W.-J. Jian, R. Santhanam, Thin Solid Films 374 (2000) 85–91.
[3] Y.L. Lo, B.J. Hwang, Langmuir 14 (1998) 944–950.
[4] G. Li, H. Li, Y. Mo, L. Chen, X. Huang, J. Power Sources 104 (2002) 190–194.
[5] H. Li, Y. Mo, N. Pei, X. Xu, X. Huang, L. Chen, J. Phys. Chem. B 104 (2000) 8477–8480.
[6] S.A. Freunberger, Y. Chen, Z. Peng, J.M. Griffin, L.J. Hardwick, F. Barde, P. Novak, P.G. Bruce, J. Am. Chem. Soc. 133 (2011) 8040–8047.
[7] R. Schmitz, R. Ansgar Müller, R. Wilhelm Schmitz, C. Schreiner, M. Kunze, A. Lex-Balducci, S. Passerini, M. Winter, J. Power Sources 233 (2013) 110–114.
[8] Z. Peng, S.A. Freunberger, Y. Chen, P.G. Bruce, Science 337 (2012) 563–566.
[9] K.W. Schroder, H. Celio, L.J. Webb, K.J. Stevenson, J. Phys. Chem. C 116 (2012) 19737–19747.
[10] P. Verma, P. Maire, P. Novák, Electrochim. Acta 55 (2010) 6332–6341.
[11] J.F. Li, S.B. Li, J.R. Anema, Z.L. Yang, Y.F. Huang, Y. Ding, Y.F. Wu, X.S. Zhou, D.Y. Wu, B. Ren, Z.L. Wang, Z.Q. Tian, Appl. Spectrosc. 65 (2011) 620–626.
[12] J.F. Li, Y.F. Huang, Y. Ding, Z.L. Yang, S.B. Li, X.S. Zhou, F.R. Fan, W. Zhang, Z.Y. Zhou, D.Y. Wu, B. Ren, Z.L. Wang, Z.Q. Tian, Nature 464 (2010) 392–395.
[13] C.K. Chan, H. Peng, G. Liu, K. McIlwrath, X.F. Zhang, R.A. Huggins, Y. Cui, Nat. Nanotechnol. 3 (2007) 31–35.
[14] L. Chen, K. Wang, X. Xie, J. Xie, J. Power Sources 174 (2007) 538–543.
[15] S.-L. Chou, J.-Z. Wang, M. Choucair, H.-K. Liu, J.A. Stride, S.-X. Dou, Electrochem. Commun. 12 (2010) 303–306.
[16] H. Ota, Y. Sakata, A. Inoue, S. Yamaguchi, J. Electrochem. Soc. 151 (2004) A1659.
[17] M. Holzapfel, H. Buqa, L.J. Hardwick, M. Hahn, A. Würsig, W. Scheifele, P. Novák, R. Kötz, C. Veit, F.-M. Petrat, Electrochim. Acta 52 (2006) 973–978.
[18] J. Nanda, M.K. Datta, J.T. Remillard, A. O'Neill, P.N. Kumta, Electrochem. Commun. 11 (2009) 235–237.
[19] M.H. Brooker, J.B. Bates, J. Chem. Phys. 54 (1971) 4788–4796.
[20] P. Pasierb, S. Komornicki, M. Rokita, M. Rekas, J. Mol. Struct. 596 (2001) 151–156.
[21] B. Fortunato, P. Mirone, G. Fini, Spectrochim. Acta Part A Mol. Spectrosc. 27 (1971) 1917–1927.
[22] Y. Wang, S. Nakamura, K. Tasaki, P.B. Balbuena, J. Am. Chem. Soc. 124 (2002) 4408–4421.
[23] P. Larkin, in: P. Larkin (Ed.), Infrared and Raman Spectroscopy, Elsevier, Oxford, 2011, pp. 73–115.
[24] L. El Ouatani, R. Dedryvere, C. Siret, P. Biensan, D. Gonbeau, J. Electrochem. Soc. 156 (2009) A468.
[25] L. El Ouatani, R. Dedryvere, C. Siret, P. Biensan, S. Reynaud, P. Iratcabal, D. Gonbeau, J. Electrochem. Soc. 156 (2009) A103.
[26] M.-Q. Li, M.-Z. Qu, X.-Y. He, Z.-L. Yu, J. Electrochem. Soc. 156 (2009) A294.